

Predicting the final size of small vesicles produced by pressure extrusion through nano-channels

Martin Bertrand and Béla Joós*

Received Xth XXXXXXXXXXXX 20XX, Accepted Xth XXXXXXXXXXXX 20XX

First published on the web Xth XXXXXXXXXXXX 200X

DOI: 10.1039/b000000x

Using results from a prior experimental study [Patty, P. and Frisken, B., *Biophys. J.*, **85**, 2003], we show that, to a first approximation independent of pressure, the final size of small vesicles, or liposomes, produced by pressure extrusion through nano-channels can be predicted by a simple geometrical argument that considers an invariable inner vesicle volume enclosed by a finitely extensible lipid bilayer. Our prediction is improved by arguing that the effective pore radius decreases with increasing pressure due to a thickening of the lubrication layer between the vesicles and the channel wall. We fit the experimental data with only one free parameter linked to the finite extensibility of the bilayer membrane. Finally, key elements of the model are confirmed by large scale coarse-grained molecular dynamics simulations of the pressure extrusion of lipid bilayer vesicles.

1 Introduction

Small lipid bilayer vesicles, or liposomes, are often synthesised for research and pharmacological applications^{1–3}. One of the most popular techniques to produce such soft objects is the pressure extrusion of a vesicle solution through an array of nano-channels^{2,4–7}. Related to this procedure, a long standing goal has been to be able to predict the average final size of the produced liposomes given the parameters of the system which are: lipid nature, lipid concentration, temperature, applied pressure, and radius of the channels. Two models have been proposed: the first by Clerc and Thompson⁸ refers to the Rayleigh instability⁹ and predicts a final vesicle size larger than observed^{5–7} and mostly independent of pressure; the second by Patty and Frisken⁷ uses the analogy of blowing a bubble through a hole to describe the initial entry of large vesicles in the smaller nano-channels and derives a prediction from an analysis of the phenomenon in static equilibrium. Although this last model successfully fits their data, it requires two free parameters that are not clearly linked to the physics of vesicle pressure extrusion and looks at the problem from a static viewpoint whereas our model includes a rheological description of this dynamic phenomenon.

In the final few passages of pressure extrusion, we can assume vesicles flow in and out without breaking and their shape goes back and forth between a spheroid outside of the channels and a sphero-cylinder inside. With equal volume, the sphero-

cylinder has a greater area than the sphere. Therefore the final vesicles are of a size such that the lipid bilayer can tolerate this area difference. We show that to a first approximation, this prediction is valid. We then incorporate the effects of pressure in our simple geometrical argument using elements of a model of sphero-cylindrical vesicles flowing in narrow channels developed by Bruinsma¹⁰ to predict the final sizes of extruded vesicles as pressure is increased. This idea was mentioned by Hunter and Frisken⁵ but not exploited. Flow being involved here, it comes to no surprise that the length of the channels is an important parameter in our model which goes against results reported by Frisken *et al.*⁶: they show that at low pressures, doubling the length of the channels does not significantly influence the final sizes of the produced vesicles. We propose that this measurement should be repeated at higher pressures as our model predicts much change in that regime while it corroborates experimental evidence at lower pressures. Our model can also explain the dependence in lipid concentration observed⁶.

We also use out of equilibrium coarse-grained molecular dynamics simulations of vesicle extrusion to confirm our geometrical argument, to corroborate some main elements of Bruinsma's theory¹⁰, and to describe the initial entry of a large vesicle in a nano-channel and its subsequent rupture. Although the extrusion of vesicles¹¹ and erythrocytes¹² has been simulated in the past, to the best of our knowledge no true bilayer vesicle in an explicit solvent has ever been simulated in such a context. We leverage the computing power of Graphical Processing Units (GPUs) to make this feasible in a relatively

*Department of Physics, University of Ottawa, 150 Louis-Pasteur, Ottawa, Canada, K1N 6N5. Tel: 1 (613) 568-5800; E-mail: bjooos@uottawa.ca

short time frame.

Our model and study should be useful to experimentalists considering pressure extrusion as a means to produce liposomes, but also to the large community studying the flow of diverse cells in and out of narrow channels such as red blood and plasma cells flowing in narrow capillaries.

2 Extrusion model

The production of liposomes through pressure extrusion consists in starting with a solution of large and possibly multilamellar vesicles (MLVs) that is pushed by a pressure drop ΔP multiple times through an array of nano-channels of average radius R_p and length L_p as seen in Fig. 1 (typically 10-15 times⁵⁻⁷). For every passage through the extruder there is an ever diminishing drop in the average vesicle size (see Fig. 1 in the article by Frisken *et al.*⁶). Thus, towards the end of the entire extrusion procedure, most vesicles in solution flow in and out of the nano-channels without rupturing. To a first approximation, we assume that in these last passages they transition from a relatively spherical shape outside the nano-channels to a sphero-cylindrical shape inside and back again while conserving volume as depicted in Fig. 1. Let us develop this argument.

2.1 Surface and volume conservation

We start with a vesicle of apparent initial spherical area $A_0 = 4\pi R_0^2$ enclosing a volume $V_0 = 4\pi R_0^3/3$. The membrane tension γ is related to its fractional surface expansion $\alpha = \Delta A/A_0$ by:

$$\alpha = \frac{k_b T}{8\pi k_c} \ln \left(1 + c \frac{\gamma A}{k_c} \right) + \frac{\gamma}{K_A}, \quad (1)$$

where K_A is the area compressibility, k_c , the bending rigidity, and $c \simeq 0.1$ is a constant related to surface undulations around 0.1¹³. For high enough tension, $\gamma \simeq K_A \alpha$. Let us assume that in the extrusion process the vesicle volume stays constant while its area expands. Then there exists a critical value α_c where the vesicle ruptures. This critical surface expansion α_c can have two contributions: 1) α_A related to the flattening of the excess area in the membrane; 2) α_γ related to the lysis tension in the bilayer which depends on the nature of the lipids. Thus $\alpha_c = \alpha_A + \alpha_\gamma$.

If the vesicle is pushed almost quasistatically in a nano-channel of radius R_p , it will do so without breaking as long as the surface expansion remains below a threshold characterized by α_c . Assuming the steady-state shape in the pore to be that of a sphero-cylinder of side length L_c and radius R_p (see Fig. 1 with $h = 0$) we can find the critical vesicle to pore size ratio $R = R_0/R_p$ for which the vesicle barely remains intact by

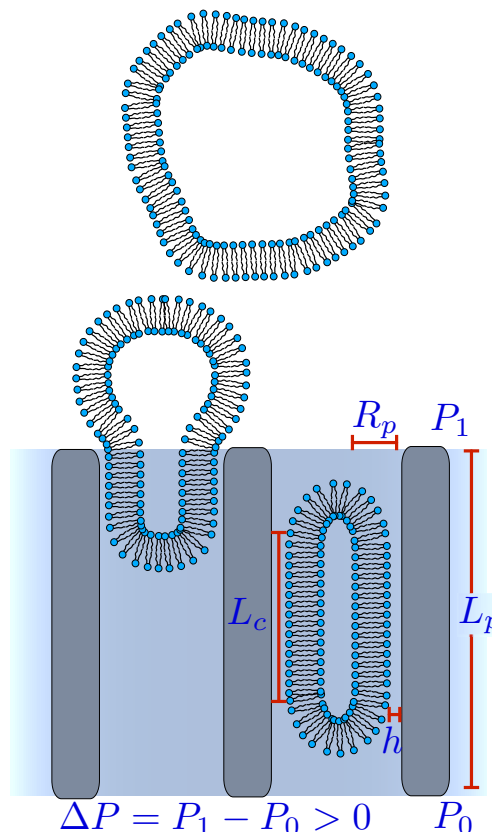


Fig. 1 In the final passages, vesicles flow through the extruder back and forth going from a roughly spherical shape outside to a sphero-cylindrical shape inside. Some key variables are highlighted.

solving the following derived polynomial:

$$V_0 = \frac{4\pi R_0^3}{3} = \pi L_c R_p^2 + \frac{4\pi R_p^3}{3} = V_f, \quad (2)$$

$$(1 + \alpha_c)A_0 = (1 + \alpha_c)4\pi R_0^2 = 2\pi L_c R_p + 4\pi R_p^2 = A_f, \quad (3)$$

$$2R^3 - 3(1 + \alpha_c)R^2 + 1 = 0. \quad (4)$$

Eq. 2 accounts for volume conservation and Eq. 3, for surface expansion, here assumed equal over the entire deformed vesicle. It will be shown in the results section that this model can only crudely approximate the mean final sizes of vesicles obtained by pressure extrusion. The next subsection extends it to account for the pressure dependence.

2.2 Pressure dependence

Between the surface of a sphero-cylindrical vesicle and the surface of the channel it's flowing through, there is a relatively thin lubrication layer of thickness h (see Fig. 1 and inset of Fig. 4 for a close-up) that grows with increasing vesicle ve-

locity U . The vesicle essentially travels in a pore of effective radius $R_{\text{eff}} = R_p - h$ that decreases with U and solving Eq. 4 in this case gives the ratio $R' = R_0/R_{\text{eff}}$. Thus if we wish to get the corrected ratio $R = R_0/R_p$ for a given applied pressure ΔP we first need to calculate h . Bruinsma has given an expression for h as a function of U ¹⁰:

$$h \cong 2.05R_p \left(\frac{\eta U}{\gamma_f} \right)^{2/3}, \quad (5)$$

where η is the solvent's viscosity and γ_f is the frontal membrane tension of the vesicle. The membrane tension γ is predicted to be linearly decreasing along the cylindrical part of the travelling sphero-cylindrical vesicle going from γ_f at the front cap ($z = 0$) to γ_r at the rear cap ($z = L_c$) such that:

$$\gamma(z) = \gamma_f - \frac{\eta U}{h(U)} z. \quad (6)$$

However, we will assume a uniform mean tension $\bar{\gamma}$ along the length of vesicle to simplify our calculations. Supposing that the vesicles flowing back and forth in the extruder can only barely support it without rupturing, we make $\bar{\gamma} = \gamma_l$ the lysis tension. Bruinsma also developed a Darcy type law to describe the flow of sphero-cylindrical vesicles in narrow channels which goes like:

$$\eta U = K' \frac{\Delta P}{L_p} = \frac{R_p^2/8}{1 + nR_p L_c(U)/4h(U)} \frac{\Delta P}{L_p}, \quad (7)$$

or equivalently for all intended purposes:

$$\eta U = K' \frac{\Delta P}{L_p} = \frac{R_p^2}{8 + 0.223nL_c(U)^3/R_p^2} \frac{\Delta P}{L_p}, \quad (8)$$

where n is the number of vesicles per unit length in the pore.

The calculation of the ratio R at a given pressure ΔP is done self-consistently using Eq. 8 for the velocity U (we get the same answers with Eq. 7):

$$R(R_p, \Delta P, \alpha_c) = \{$$

1. Calculate R' by solving Eq. 4 for a given α_c
2. Estimate L_c using Eq. 2
3. Estimate h using Eqs. 5 and 8
4. Calculate $R_{\text{eff}} = R_p - h$
5. Improve L_c using $R_p = R_{\text{eff}}$ with R' in Eq. 3
6. Improve h using the new value of L_c
7. Repeat steps 3 to 5 until h and L_c converge
8. Get R from h and R' }

(9)

3 Model agreement with experiment

Let us consider vesicles made of POPC lipids such as in Patty and Frisken's study⁷ with $K_A \cong 234\text{mN/m}$, $k_c \cong 1.43 \times 10^{-19}\text{J}$, $\gamma_l \cong 7.4\text{mN/m}$, and $R_0 = [25, 100]\text{nm}$. Using Eq. 1 we find $\alpha_\gamma \cong 0.04$. Solving Eq. 4 with this value for α_c gives $R = 1.23$ regardless of pore size or pressure. In Fig. 2 we reproduced data that originate from pressure extrusion experiments performed by Patty and Frisken on POPC lipid vesicles⁷. Our value of R predicts the smallest vesicle sizes obtained by extrusion under strong pressure gradients whereas we would have expected a better prediction for the final sizes under the weakest pressures. With $\alpha_c \cong 0.10$ we achieve this. Consequently, the final vesicles must be deflated with an excess area accounting for roughly 6% of the observed expansion ($\alpha_A \cong 0.06$) which is confirmed by the swelling they undergo at the end of the extrusion runs²¹. Although quite simplistic, we are convinced that our geometrical argument shows that to predict the final sizes of extruded vesicles one needs to describe how these objects flow through nano-channels.

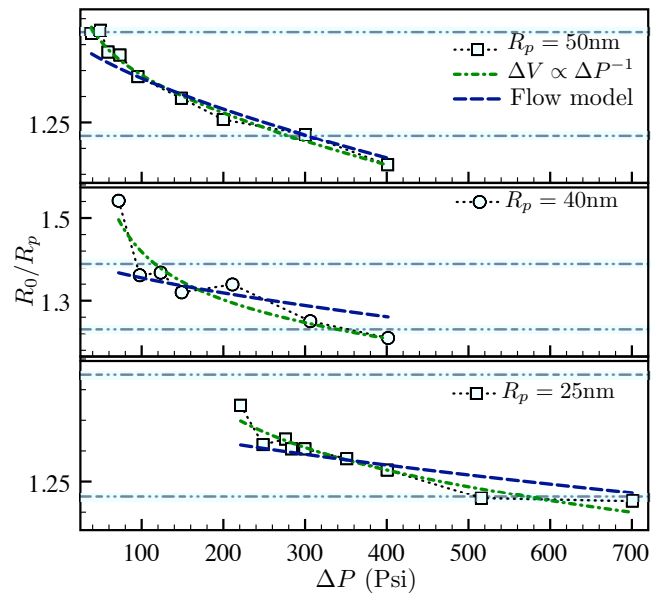


Fig. 2 Experimental data of final vesicle sizes expressed in terms of the ratio $R = R_0/R_p$ as a function of the pressure drop ΔP for three different channel sizes are reproduced from Patty and Frisken's paper⁷. The horizontal grey dot-dashed lines are those for $\alpha_c = 0.04$ at $R = 1.23$ and $\alpha_c = 0.10$ at $R = 1.39$. The blue dashed lines represent the fits of our flow model, while the green dot-dashed lines are those with the volume relaxation argument included.

We fitted Eq. 9 to data from Patty and Frisken's paper⁷. We let α_c be a free parameter and use all other parameters therein ($\gamma_l \cong 7.4\text{mN/m}$, $L_p = 6\mu\text{m}$) except n that we fix to a value of $10/L_p \cong 1.67 \times 10^{-6}\text{m}^{-1}$, roughly the number of vesicles that

can fit in the pore without affecting each other corresponding to a low initial lipid concentration. Fig. 2 shows the best fits and Table 1 gives the values for α_c as a function of the channel radius. The fits are in good agreement with the data. All expansion coefficients compare favourably with one another and are close to the upper limit $\alpha_c = 0.10$ considered in the geometrical argument for vesicles slightly deflated with some excess area. Our model seems to fail properly predicting the ratio R for the very lowest pressures especially for $R_p = 40\text{nm}$. We think this is where one needs to pay careful attention to the first few passages in the extruder. It's quite possible that at lower pressures, the probability of forming large deflated vesicles with much excess area and reduced volume is greater. To account for this in our model we can potentially relax the volume by introducing a $\Delta V \propto \Delta P^{-1}$ which allows to better fit the data, but by doing so we need to introduce a free parameter hard to relate to the actual physics in the system. We show the resulting fits on Fig. 2 for the sake of completeness although we will not further use this volume relaxation argument in the following discussion.

Table 1 The mean critical surface expansion α_c obtained while fitting data from Patty and Frisken's paper⁷ is roughly 0.10.

Channel radius R_p (nm)	Critical surface expansion α_c
25	0.083 ± 0.003
40	0.110 ± 0.005
50	0.104 ± 0.003

We took our flow model with the values of α_c we obtained and doubled the length L_p of the channels as in the paper by Frisken *et al.*⁶ where they report no significant change in the final vesicle sizes at low pressures. Given the experimental uncertainties, we show in Fig. 3 (top plot) that our model recovers that result. However, we predict that at higher pressures vesicle sizes strongly depend on the channels' length or flow if one prefers as they are related. In fact, if the reduced vesicle size R is plotted in function of $Q/K = \Delta P/L_p$, the theoretical predictions in Fig. 3 collapse onto a single curve. We therefore suggest to revisit the channel length doubling experiment at higher pressures to test the validity of our model. Interestingly, our model can also explain a result reported in the same paper⁶, that is the final sizes of vesicles weakly depend on the lipid concentration one starts with, they are slightly bigger for higher concentrations. A higher initial lipid concentration should result in more vesicles flowing in a given channel at the same time. We thus increased n ten fold in our model which then predicts a slight increase in the average vesicle size as expected (see Fig. 3, bottom plot).

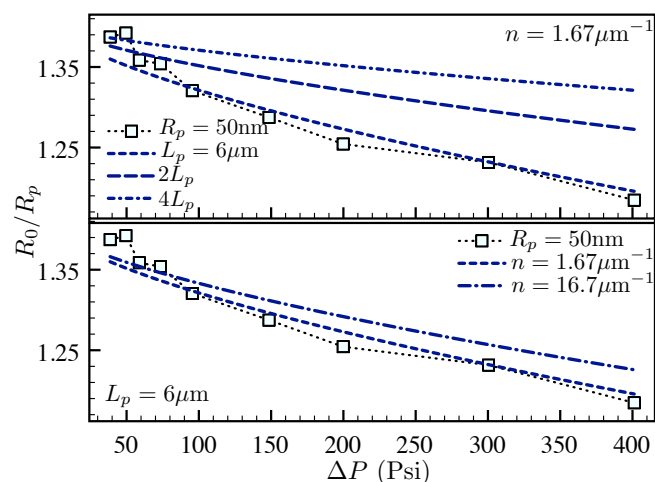


Fig. 3 Top plot: while doubling or even quadrupling the channel length does not change much the final vesicle sizes at lower pressures which corroborates previous findings⁶, the difference is much more important at higher pressures. Bottom plot: Increasing the initial lipid concentration inevitably increases the number of vesicles in a given channel and thus n which results in slightly bigger final vesicles as previously observed⁶.

4 CGMD simulations of the extrusion process

Our flow model presented in Sect. 2 predicts the final sizes of extruded vesicles based on an analysis of the last few passages in a pressure extrusion run where size is expected to vary only marginally. It combines a geometrical argument (Sect. 2.1) to elements of Bruinsma's description of spherocylindrical vesicles flowing down narrow channels (Sect. 2.2). Using a Coarse-Grained Molecular Dynamics (CGMD) model, we thus decided to simulate small inflated and spherical lipid bilayer vesicles being pressure extruded in channels of different sizes to corroborate qualitatively if not quantitatively the various components of our model (Sect. 4.1). We also simulated larger vesicles extruded in the same narrow channels to give a qualitative description of the initial extrusion passages (Sect. 4.2).

In our CGMD simulations of lipid bilayer systems, we modelled all interactions using Goetz and Lipowsky's set of potentials¹⁴ where σ is the unit of length, ϵ , of energy, τ , of time, and m , of mass. We used lipids with one bead for the hydrophilic head and two beads for the hydrophobic tail. The lipids are fully flexible with no bending potential along their length. The hydrophilic solvent is of the Lennard-Jones (LJ) type with a density of $0.8\sigma^{-3}$. We characterized bilayers made of these short lipids and immersed in such a solvent at a temperature $k_B T = 1.0\epsilon$ (data not shown). From the calculation of the microscopic stress tensor¹⁴, we found $\alpha_0 \cong 1.9\sigma^2$, the area per lipid at which the stress is zero

with a bilayer thickness $l_{\text{BM}} \cong 4.8\sigma$, and an area compressibility $K_A = 8.84 \pm 0.76\epsilon/\sigma^2$. We then calculated the bending rigidity using its relation to the area compressibility¹⁵ $k_c = K_A l_{\text{BM}}^2/48 = 4.24 \pm 0.36\epsilon$. As expected, our membranes are softer than those studied by Goetz and Lipowsky made of lipids with longer tails in a solvent of lower density at a slightly higher temperature^{14,15}.

For the simulations of lipid bilayer vesicle pressure extrusion we constructed a system made of two reservoirs linked by a channel of radius R_p and length L_p . The vesicle started in one of the reservoirs and a pressure drop was applied across the system such that it penetrated the pore, travelled along its length, and ended up in the second reservoir. The walls consisted in solvent beads laid out on an FCC lattice with density $1.0\sigma^{-3}$ and anchored in space with stiff harmonic springs¹⁶. We used DPD interactions to thermostat the system to a thermal energy $k_B T = 1.0\epsilon$ as they allow for momentum propagation¹⁷, an essential feature to study flows (out of equilibrium dynamics).

The simulations, which contained from a quarter to half a million particles in total, were initialized using the ESPResSo package¹⁸ executed on Graphical Processing Units (GPUs) using a customized version of the very fast and optimized HOOMD-Blue package^{19,20}. Simulations ran on Sharcnet's Angel cluster which contains 44 NVIDIA Tesla 1070 GPUs. Of course, even with a decent amount of computation power it always remained beyond our ability to simulate a solution of vesicles pressure extruded multiple times. But we can learn much from the study of the extrusion of a single vesicle.

4.1 Final passages simulated

The extrusion in nano-channels of small vesicles made of $n_l = 3000$ lipids was simulated. Vesicles were all initially set up such that the bilayer was under no stress due to a pressure difference between the inside and the outside (Fig. 7A). The outer layer was made of $n_{\text{out}} = 1841$ lipids with a mean area per lipid head $a_{\text{out}} = 1.86\sigma^2$ which corresponds to a radius of $R_{0,\text{out}} = 16.5\sigma$ while the corresponding values of the inner layer $n_{\text{in}} = 1159$, $a_{\text{in}} = 1.68\sigma^2$, and $R_{0,\text{in}} = 11.5\sigma$. The inner layer thus started more compressed than the outer layer. This is a consequence of requiring the area per lipid to be constant as measured in the mid-section of the bilayer ($a_{\text{mid}} \approx 1.75\sigma^2$). Overall the area per lipid of our vesicles is smaller than $a_0 = 1.9\sigma^2$ found for flat bilayer membranes. This is mainly due to the difference in geometry in the finite size of our systems.

4.1.1 Geometrical argument. We tracked multiple observables throughout our simulations one of the most important being the local area per lipid a which is directly related to the stress in the bilayer. It was calculated from the triangulation of both the outer and inner layers using the Crust surface reconstruction algorithm²² while accounting for lipid flips

from one layer to the other. Following a and its mean \bar{a} permitted to determine both the time and the spatial coordinates of a rupture event. The observation of many such events (Fig. 7C) lead to values of the expansion coefficient for both layers very close to one another of $\alpha_{c,\text{out}} \cong \alpha_{c,\text{in}} \equiv \alpha_c \cong 0.21$. Feeding this α_c into Eq. 4 gives a ratio $R = R_0/R_p = 1.62$. Taking the initial outside radius previously given we find $R_{p,\text{crit}} = 10.2\sigma$, the smallest channel radius into which the vesicle can penetrate and travel without breaking. Now in our simulations, even at the lowest pressures, there is a lubrication layer between the vesicle and the channel wall of minimal thickness close to the size of a LJ bead $h_{\text{min}} \cong 1.1\sigma$. We thus need to compare the predicted critical radius with the minimal effective radius $R_{\text{eff}} = R_p - h_{\text{min}}$. Because our walls were set up on a lattice to maximize impermeability, we could not fine tune the radius to a very specific value, but when $R_p = 12.0\sigma$, that is $R_{\text{eff}} = 10.9\sigma$, we could barely push vesicles in without breaking them while for $R_p = 11.5\sigma$, $R_{\text{eff}} = 10.4\sigma$, it appeared impossible on the time scale of our simulations. Thus the true size limit is most probably very close to the one predicted by the geometrical argument.

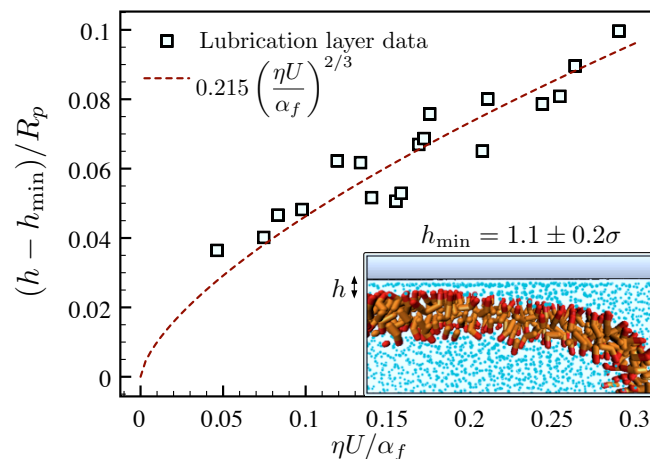


Fig. 4 The lubrication layer's thickness h grows with $\eta U/\gamma_f$ like predicted by Bruinsma¹⁰. Here we used α_f , the frontal area per lipid expansion of the outer layer of the membrane of our spherocylindrical vesicles travelling in channels that we assume goes like γ_f , the frontal tension in the membrane.

4.1.2 The lubrication layer. We measured the thickness of the lubrication layer h and can assert that it does increase with the mean flow velocity U as predicted by Bruinsma¹⁰. To our knowledge, this is the first direct measurement of h for a vesicle flowing in a narrow channel. We show in Fig. 4 the cumulative data for vesicles flowing in channels of radii $R_p = \{13.0, 13.5, 14.0\}\sigma$ plotted using non-dimensional axes $(h - h_{\text{min}})/R_p$ vs $\eta U/\alpha_f(U)$, where α_f is the frontal area per

lipid expansion of the outer layer of the vesicles, η is the appropriate shear viscosity, and $h_{\min} = 1.1 \pm 0.3$ is the minimum thickness of the lubrication layer whose value was extracted by fitting the data. One can see that the expected power law behaviour with an exponent of $2/3$ agrees very well with our data. Furthermore, the minimal thickness h_{\min} found corresponds to the approximate value we can directly extract from simulations at the lowest pressures (see Sect. 4.1.1). Fluid particles within a distance h_{\min} away from the channel wall move with a velocity roughly an order of magnitude slower than the vesicle and close to zero such that they essentially create a no-slip layer.

4.1.3 Darcy's law. The actual relationship between flow velocity and pressure may be written as $\eta U = K'(\Delta P - \Delta P_{\min})/L_p^6$ where ΔP_{\min} is the minimum pressure to push a vesicle of given size in the channel and K' is defined in Eq. 7. We plotted, in Fig. 5, ΔP as a function of UL_p/K' for data from simulations of small vesicles made of $n_l = 3000$ lipids pushed in channels of radii $R_p = \{13.0, 13.5, 14.0\}\sigma$ and extracted the shear viscosity η of the fluid in the lubrication layer and a mean minimum pressure ΔP_{\min} .

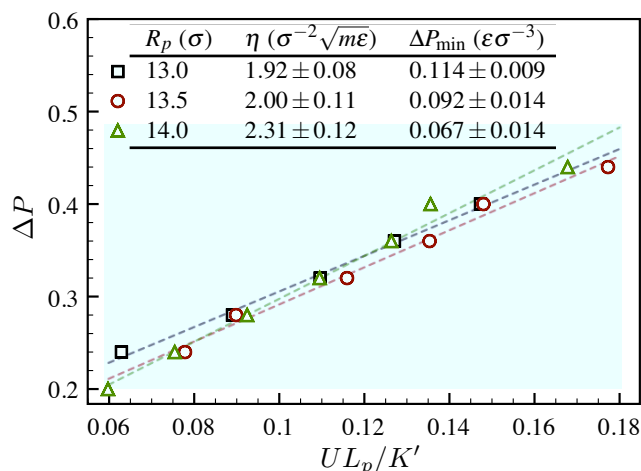


Fig. 5 Verifying that Darcy's law of the form $\eta U = K'(\Delta P - \Delta P_{\min})/L_p$ holds for our simulated vesicles. We here show linear plots of ΔP as a function of UL_p/K' for various channel radii $R_p = \{13.0, 13.5, 14.0\}\sigma$. The slope is the shear viscosity η and the intercept, the minimum pressure ΔP_{\min} .

The table at the top of Fig. 5 summarizes the results. We calculated the shear viscosity of a quiescent LJ fluid of density $\rho = 0.8\sigma^{-3}$ at temperature $k_B T = 1.0\epsilon$ using Green-Kubo's formulation²³ and found it to be $\eta = 1.98 \pm 0.16\sigma^{-2}\sqrt{m\epsilon}$ in line with²⁴. The shear viscosities reported in Fig. 5 are mostly within the margins of uncertainty of the expected value, a remarkable result given the number of parameters included in the calculation. Any small change to these produces impor-

tant deviations in the value of η . We cannot explain the apparent rise of shear viscosity with the channel radius although it could very well be a statistical artifact. As for the minimal pressure, one would expect it to decrease as the radius of the channel increases and this is what we observe. However, we were not able to directly verify the accuracy of these predicted values in our simulations due to time constraints (very long and multiple massive simulations necessary).

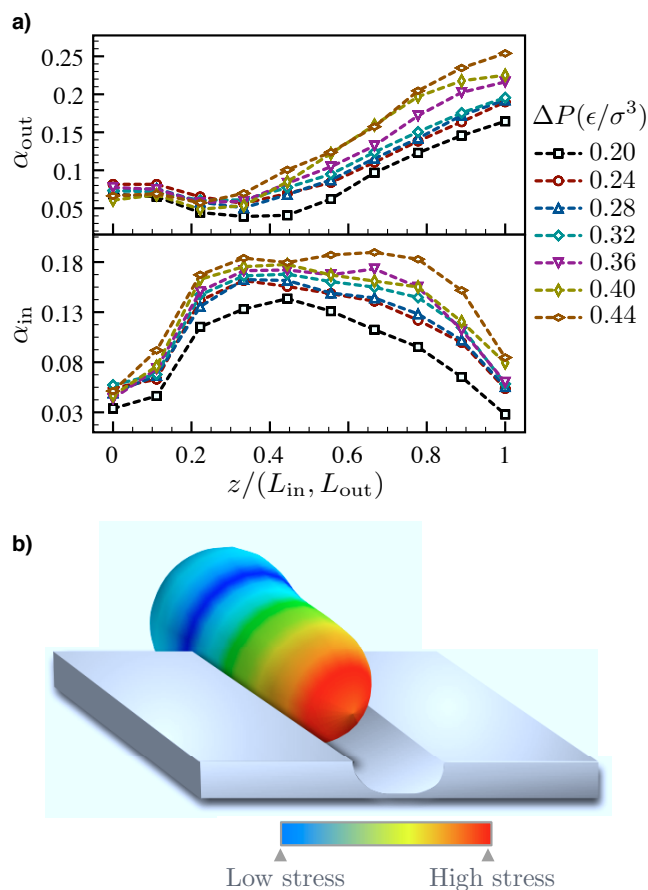


Fig. 6 a) Average tension profiles for the outer and inner layers of the membrane inferred from the change in area per lipid α as the sphero-cylindrical vesicles travel down the channel. The z coordinate along the length of the objects has been renormalized for ease of calculation and clarity. One can clearly observe, in the outer layer, the linear decrease of tension going from the frontal cap of the vesicle to its back. b) Heat map of the stress on the outer shell of the vesicle as it enters the channel: clearly pore nucleation and rupture is more probable close to the tip and along the cylindrical portion of the vesicle.

4.1.4 Tension profile along the vesicle. The frontal area expansion α_f used in verifying the validity of Eq. 5 in our simulations was obtained from profiles along the length of sphero-cylindrical vesicles such as those in Fig. 6a. Assum-

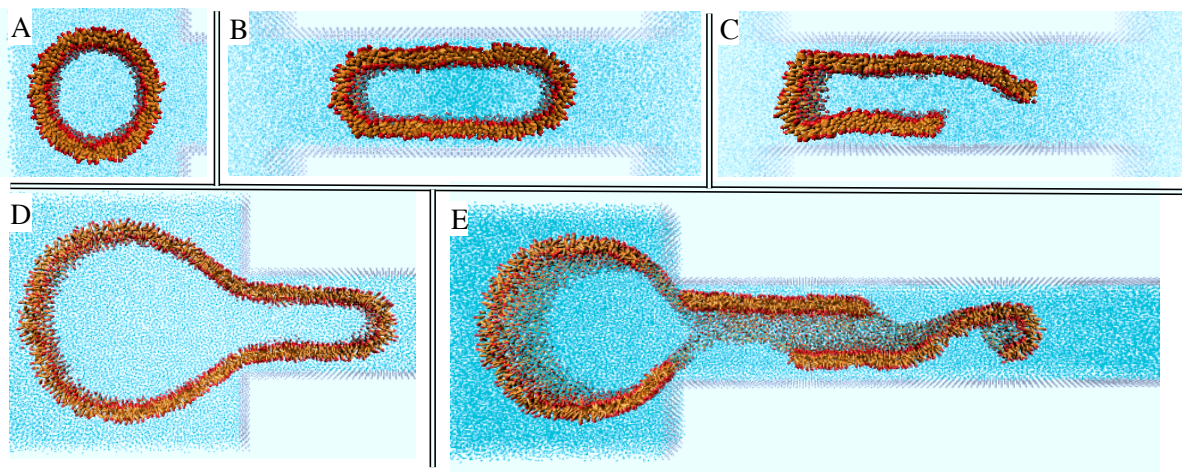


Fig. 7 Slices from 3D simulations of the pressure extrusion of vesicles in nano-channels. A) The initial shape of the vesicle for reference. B) A sphero-cylindrical vesicle flowing in the channel. C) A sphero-cylindrical vesicle breaking in a channel while pushed by a strong pressure difference. D) The typical shape of a vesicle as it is entering the channel. E) The rupture of a large vesicle at the entrance of a small channel.

ing we are in a linear regime where $\gamma \cong K_A \alpha$ we find that the profile for the outer layer of the membrane corroborates Eq. 6, that is tension decreases linearly along the cylindrical part of the vesicle in the channel going from the front to the back. The slope of the linear part should be, according to the same equation, $\eta U / K_A (h - h_{\min})$. We thus extracted from our data an approximate value for the area compressibility modulus $K_A = 8.83 \pm 0.34 \epsilon / \sigma^2$. Remarkably, it coincides with the value found for our model bilayers $K_A = 8.84 \pm 0.76 \epsilon / \sigma^2$ (Sect. 4). Fig. 6a also shows the frontal tension increasing with the velocity as expected. Interestingly, the area expansion profile for the inner layer of the membrane does not follow its outer counterpart. Indeed, the area expansion appears roughly constant along the cylindrical part of the vesicle which means the shear stresses the outer membrane is subjected to get damped in the bilayer and do not propagate to the inner heads. It's an interesting question whether this occurs or not in real nano-size vesicles flowing down narrow channels.

4.2 Initial passages simulated

To produce small vesicles by pressure extrusion, one starts with a solution of rather large vesicles that break into smaller and smaller pieces with each passage through the extruder until the size stabilizes. Until now one could only guess what is the true mechanics of rupture of these large initial vesicles. For instance, it has been proposed that the rupture occurs at the neck of the channel in an axisymmetric fashion such that small hemispherical vesicles are literally expressed from the larger ones (“blowing a bubble” model of Patty and Frisken⁷). Here we provide a first qualitative description based on evi-

dence gathered in our simulations which shows that this is not the case.

A large vesicle ($n_l = 10000$) approaching a small channel ($R_p = 12.0\sigma$) in a converging flow field eventually gets sucked-in due to the hydrodynamic friction with fluid particles speeding by as they enter the channel. Fig. 7D shows the vesicle as it is squeezing in the channel. Then one of two scenarios can happen: 1) the pressure is too weak and the vesicle reaches an equilibrium state; 2) the pressure is strong enough leading to rupture. When the vesicle ruptures, it always does so through pore nucleation whose probability is greater near the tip and decreases towards the neck as shown in Fig. 6b. Rupture often occur in multiple sites at the same time which gives rise to flowing lipid sheets along the channel as shown in Fig. 7E. The sheets can then rip apart into smaller pieces in the channel and drift towards the other end where they fold again into floppy, partly deflated smaller vesicles. We think that the slightly higher than expected values of the surface expansion coefficient α that we found while analysing results from Patty and Frisken⁷ are in part due to that loss of total internal volume or, equivalently, the creation of excess area. The polydispersity observed in the final sizes of vesicles produced by pressure extrusion⁵⁻⁷ is most probably a direct consequence of the stochastic nature of the rupture of large vesicles penetrating into channels of small opening.

5 Conclusion

Given the lysis tension γ_l and related approximate critical area expansion α_c of a lipid bilayer, the radius R_p and length L_p

of the extruder's channels, and the applied pressure ΔP , one can predict the mean final size of vesicles obtained by pressure extrusion. We combined a simple geometrical argument with elements of Bruinsma's theory about spherocylindrical vesicles travelling in a narrow channel¹⁰ to describe the flow of vesicles in the final extrusion passages. This is mainly pertinent to experimentalists as our model relies on no truly free parameter. In fact, only the critical area expansion might pose some issues as it combines both membrane expansion and consumption of excess area, the latter being hard to exactly predict without a better understanding of the initial passages of the vesicle solution in the extruder. However, if desired, it can certainly be estimated to a few percentage points. We also make some distinct predictions about the effects of lipid concentration in solution and channel length on the final vesicle sizes which should be verified experimentally.

The Molecular Dynamics part of our paper presents results from large scale non-equilibrium coarse-grained molecular dynamics simulations of nano-sized vesicles being extruded in narrow channels. Both lipids and solvent were explicitly included in the simulations, which to our knowledge is a first. The simulation cost has always been a major deterrent for doing so, but with the introduction of GPU-optimized code, it is now feasible on a reasonable time scale. One can even buy for a relatively low price a desktop workstation equipped with multiple GPUs that has the computing power of a small to medium size cluster of CPUs. The results of our simulations agree exceptionally well with Bruinsma's¹⁰ description of a spherocylindrical vesicle flowing in a narrow channel and our own geometrical argument. We also used our simulations to try and give a qualitative description of the initial passages of large vesicles in the extruder. We showed that large vesicles did not tear apart cleanly as assumed by Patty and Frisken⁷ but that ruptures occurred heterogeneously along the cylindrical part of the vesicle that is in the channel and that large sheets of lipids flow down the channel to close again into smaller and floppier vesicles.

Rupture in the channel of small extruded vesicles was frequently observed near the critical size. It is always accompanied by content loss and eventual closure of nucleated pores. A detailed study of this phenomenon will be presented in a subsequent paper. It should appeal to those interested in the encapsulation and release of drugs in the body, and to those studying the flow induced rupture of red blood cells in small capillaries since vesicles have similar rheological properties.

References

- 1 A. Jesorka and O. Orwar, *Annu. Rev. Anal. Chem.*, 2008, **1**, 801–832.
- 2 D. Fenske, A. Chonn and P. Cullis, *Toxicol. Pathol.*, 2008, **36**, 21.
- 3 B. Maherani, E. Arab-Tehrany, R. Mozafari, C. Gaiani and M. Linder, *Current Nanoscience*, 2011, **7**, 436–452.

- 4 M. Hope, M. Bally, G. Webb and P. Cullis, *Biochim. Biophys. Acta*, 1985, **812**, 55–65.
- 5 D. Hunter and B. Frisken, *Biophys. J.*, 1998, **74**, 2996–3002.
- 6 B. Frisken, C. Asman and P. Patty, *Langmuir*, 2000, **16**, 928–933.
- 7 P. Patty and B. Frisken, *Biophys. J.*, 2003, **85**, 996–1004.
- 8 S. Clerc and T. Thompson, *Biophys. J.*, 1994, **67**, 475–477.
- 9 L. Rayleigh, *Proceedings of the London Mathematical Society*, 1878, **1**, 4.
- 10 R. Bruinsma, *Physica A: Statistical and Theoretical Physics*, 1996, **234**, 249–270.
- 11 G. Gompper and D. Kroll, *Phys. Rev. E*, 1995, **52**, 4198–4208.
- 12 D. Quinn, I. Pivkin, S. Wong, K. Chiam, M. Dao, G. Karniadakis and S. Suresh, *Ann. Biomed. Eng.*, 2011, 1–10.
- 13 W. Rawicz, K. Olbrich, T. McIntosh, D. Needham and E. Evans, *Biophys. J.*, 2000, **79**, 328–339.
- 14 R. Goetz and R. Lipowsky, *J. Chem. Phys.*, 1998, **108**, 7397–7409.
- 15 R. Goetz, G. Gompper and R. Lipowsky, *Phys. Rev. Lett.*, 1999, **82**, 221–224.
- 16 F. Tessier and G. Slater, *Macromolecules*, 2005, **38**, 6752–6754.
- 17 T. Soddemann, B. Dünweg and K. Kremer, *Phys. Rev. E*, 2003, **68**, 046702.
- 18 H. Limbach, A. Arnold, B. Mann and C. Holm, *Comput. Phys. Commun.*, 2006, **174**, 704–727.
- 19 J. Anderson, C. Lorenz and A. Travesset, *J. Comput. Phys.*, 2008, **227**, 5342–5359.
- 20 A. Anderson, J and A. Travesset, *Comput. Sci. Eng.*, 2008, **10**.
- 21 B. Mui, P. Cullis, E. Evans and T. Madden, *Biophys. J.*, 1993, **64**, 443–453.
- 22 N. Amenta, M. Bern and M. Kamvysselis, *Proceedings of the 25th annual conference on Computer graphics and interactive techniques*, 1998, 415–421.
- 23 M. Kenward and G. Slater, *Eur. Phys. J. E*, 2004, **14**, 55–65.
- 24 K. Meier, A. Laesack and S. Kabelac, *J. Chem. Phys.*, 2004, **121**, 3671.